Int J Adv Manuf Technol (2010) 48:213–226
DOI 10.1007/s00170-009-2260-z

ORIGINAL ARTICLE

Prediction of surface roughness and dimensional deviation of workpiece in turning: a machine vision approach

H. H. Shahabi · M. M. Ratnam

Received: 10 April 2009 / Accepted: 9 July 2009 / Published online: 27 August 2009

Abstract In the past, roughness values measured directly on machined surfaces were used to develop mathematical models that are used in predicting surface roughness in turning. This approach is slow and tedious because of the large number of workpieces required to obtain the roughness data. In this study, 2-D images of cutting tools were used to generate simulated workpieces from which surface roughness and dimensional deviation data were determined. Compared to existing vision-based methods that use features extracted from a real workpiece to represent roughness parameters, in the proposed method, only simulated profiles of the workpiece are needed to obtain the roughness data. The average surface roughness R_a, as well as dimensional deviation data extracted from the simulated profiles for various feed rates, depths of cut, and cutting speeds were used as the output of response surface methodology (RSM) models. The predictions of the models were verified experimentally using data obtained from measurements made on the real workpieces using conventional methods, i.e., surface roughness tester and a micrometer, and good correlation between the two methods was observed.

Keywords Prediction · Design-of-experiment · Surface roughness · Dimensional deviation · Machine vision

H. H. Shahabi · M. M. Ratnam (✉)
School of Mechanical Engineering, Engineering Campus,
Universiti Sains Malaysia,
14300 Nibong Tebal, Penang, Malaysia
e-mail: mmaran@eng.usm.my

1 Introduction

The surface quality and dimensional accuracy of a finished workpiece are equally important in determining its performance in service. The ability to predict the surface quality even before machining based on the input variables, such as cutting speed, feed rate, depth of cut, etc., will give manufactures an advantage in terms of cost saving, shorter cycle time, and less re-work or rejects. This capability, if built into automated machines, could also lead to better-quality products and increases in productivity.

Extensive works have thus been reported over the last two decades in predicting the surface quality of workpieces for a given set of machining parameters and tool conditions. Benardos and Vosniakos [1] reviewed more than 40 papers on the prediction of surface roughness. Lu [2] reviewed several methodologies employed for the prediction of surface profile and roughness and presented the author's own work on the prediction of surface profile using the RBF neural network.

In order to develop a methodology to predict the surface roughness, two general approaches have been attempted previously. In one approach, the response surface methodology (RSM) in combination with design of experiment (DoE) or regression analysis is used to develop a mathematical model for predicting the surface roughness for a given set of input parameters. For instance, Cakir et al. [3] studied the effects of cutting parameters on the surface roughness through mathematical models developed using a series of turning experiments. Fifty-four experiments were conducted using chemical vapor deposition (CVD) and physical vapor deposition (PVD) coated tools, and the surface roughness parameter R_a on each workpiece was measured. Regression analysis using least squares method was used to develop linear, second-order, and exponential

models. Choudhury and El-Baradie [4] used RSM to develop first- and second-order surface roughness prediction equations. Each experiment was started with a new cutting tool and the surface roughness was measured using the tactile roughness tester. Arbizu and Pérez [5] used factorial design with regression techniques to develop first-order linear and second-order polynomial models to predict surface roughness. A similar study was carried out by Dabnun et al. [6] in the turning of a glass–ceramic composite.

In another approach, artificial intelligence methods, particularly neural networks, have been applied to predict the surface roughness based on the input variables. Karayel [7] developed a feed-forward, multi-layered neural network that takes depth of cut, cutting speed, and feed rate as input parameters to predict the surface roughness in a CNC lathe. Thirty-five experimental data were used to train the network. A control algorithm was also developed to determine the cutting parameters for the desired roughness value. Risbood et al. [8] used neural network to predict surface roughness and dimensional deviation of the workpiece by using the radial acceleration of the tool holder vibration as feedback.

Although many researchers in the past achieved varying degrees of success in predicting the surface roughness, both approaches required extensive experimental work to collect data in developing the models or training the neural networks. In most cases, the roughness values were measured directly using the standard stylus-type (tactile) roughness testers after machining the workpiece. The data are then used to develop the models.

In recent years, the development of machine vision hardware and advanced image processing technology has opened up new possibilities in the field of tool condition monitoring. Several researchers employed machine vision and other optical methods to obtain data that were used in surface roughness prediction. For instance, Lee and Tarng [9] predicted the surface roughness in a turning operation using features extracted from images of the workpiece surface using a polynomial network. The feature extracted was the arithmetic average of the gray level intensity of the image. The polynomial network, based on a self-organizing adaptive modeling method, was applied to predict the actual surface roughness of the workpiece using the feature. Lee et al. [10] used a vision system to predict the surface roughness of the workpiece using an abductive network. Two features obtained from the captured images, namely principal component magnitude squared and standard deviation of gray level of images, were used as the input of the network to predict R_a as the output parameter. Ho et

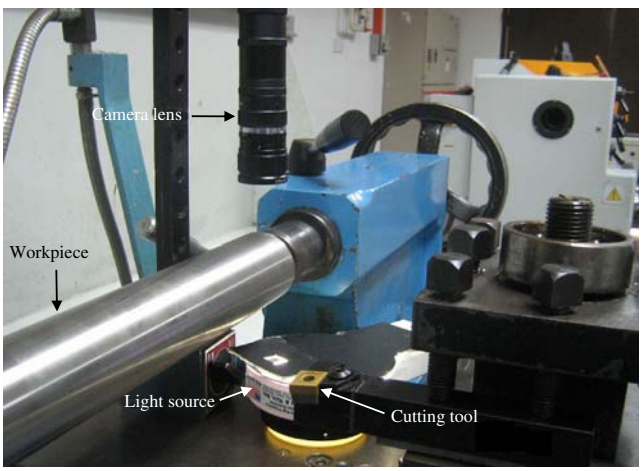

Fig. 1 Set-up for in-cycle surface roughness and tool wear measurement

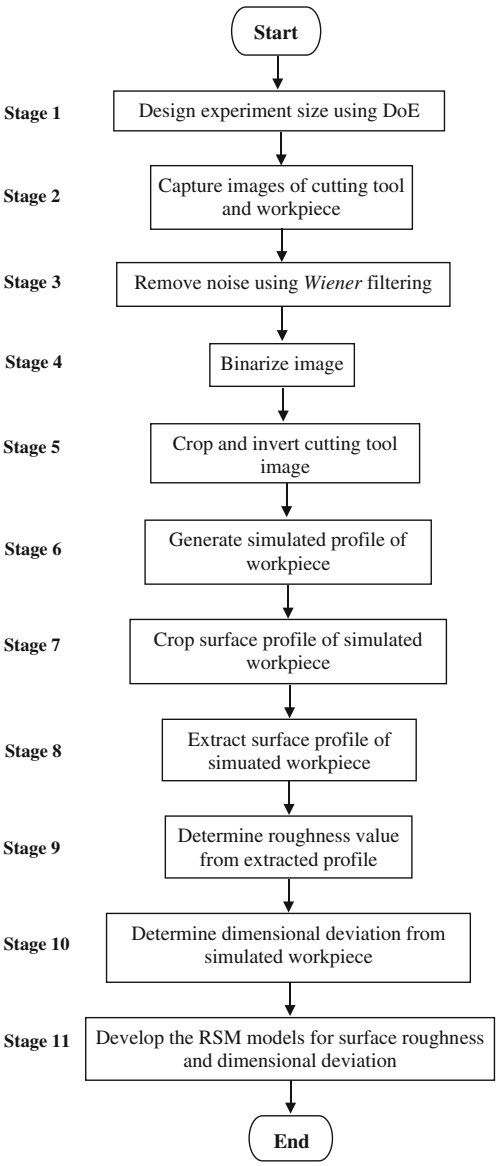

Fig. 2 Flowchart of algorithm

Table 1 Variables and levels in the DoE

	Low	Center	High
Coding	−1	0	1
Cutting speed (m/min)	170	188	206
Feed rate (mm/rev)	0.2	0.25	0.3
Depth of cut (mm)	0.15	0.2	0.25
Machining duration (min)	0	2.5	5

al. [11] proposed a method to predict the surface roughness using a machine vision approach. Their method was based on a neuro-fuzzy system that was able to predict the actual surface roughness using machining parameters and features of surface images. Lee et al. [12] established a model to predict R_a based on an adaptive neuro-fuzzy inference system (ANFIS). This method was based on features obtained from the images captured, i.e., spatial frequency, arithmetic mean value, and standard deviation of gray levels, without using the machining parameters. All the machine vision approaches proposed in the past also required preparation of the real samples used in developing the models.

One of the main advantages of the machine vision method is that the images captured can be easily manipulated or analyzed digitally to obtain the desired effects or extract the required features. In our recent work [13], the workpiece surface roughness was determined from the 2-D image of the surface profile captured at high resolution with the aid of backlighting. This method was proven to be accurate when compared to the standard stylus-type roughness tester. The advantages of the machine vision method in turning studies are that (1) it enables the measurement of surface roughness to be carried out without removing the workpiece from the lathe, (2) the measurement can be done rapidly at different parts of the workpiece, and (3) it is non-contacting. If a high-resolution camera is used, the vision method of roughness measurement on turned parts could be even more accurate than the stylus method because every point on the surface profile is used for roughness calculation, while the accuracy of the stylus method is limited by the probe tip radius (2–3 μm) and the sampling frequency of the instrument.

The potential of the machine vision method is extended further in this work for the prediction of surface roughness and dimensional deviation of the workpiece for different machining conditions. Unlike the conventional (non-vision based) methods used in the past for surface roughness prediction, the possibility of using only the 2-D image of the cutting tools (new or worn) for generating simulated workpiece profiles from which roughness data are extracted is demonstrated. Although roughness prediction is well studied and reported, the prediction of both roughness and dimensional deviation of the workpiece was reported by only a few researchers, e.g., [8].

2 System set-up

Figure 1 shows a photograph of the hardware used to capture the images of cutting tool and surface profile of the workpiece. A high-resolution (1,296×1,024 pixels) CCD camera (model JAI CV-A1), a 50-mm lens, a 220-mm extension tube, a Data Translation (DT3162) frame grabber, and a Pentium IV (2 GHz) personal computer were used to capture and digitize the images. A diffused backlight was

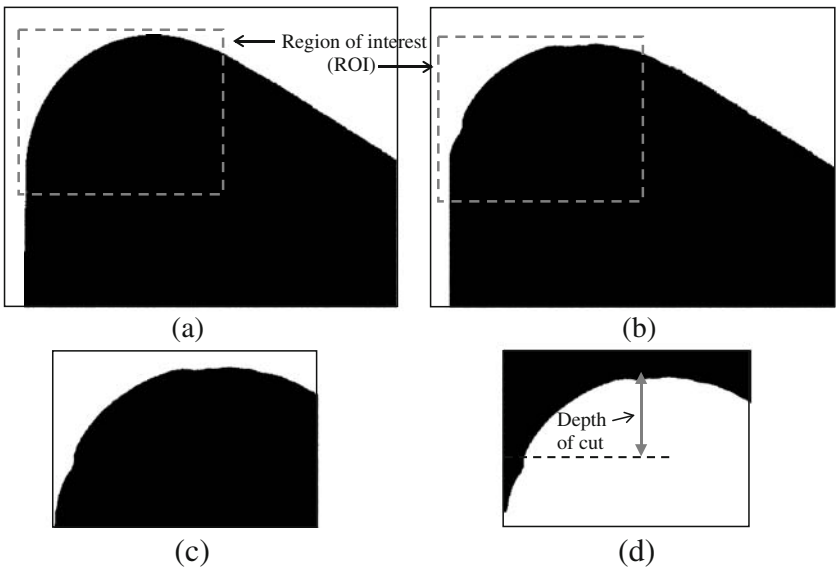

Fig. 3 **a** Unworn cutting tool tip, **b** worn cutting tool tip after 5 min of machining, **c** ROI of worn tool, and **d** inverted image

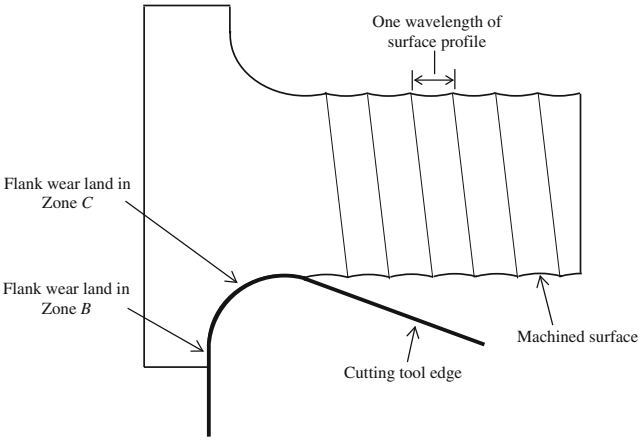

Fig. 4 2-D schematic shape of workpiece produced on a lathe

used to highlight the contour of the cutting tool. The horizontal and vertical scaling factors for the output images were determined using a high-resolution Ronchi ruling (200 line/mm) supplied by Edmond Optics. The horizontal and vertical scaling factors are 0.93 and 1 μm/pixel, respectively. The field of view of the lens is 1.2 by 1.0 mm.

The machine tool used was a conventional lathe machine (Pinacho S90/200, Spain). A 70-mm-diameter AISI 304 stainless steel rod was used as the workpiece, which was machined using uncoated carbide cutting tools (CNGP-12-04-04_H13A) manufactured by Sandvik, Sweden. The cutting tools were selected from the *G* class due to their closer tolerance. The cutting speed, feed rate, depth of cut, and duration of machining were changed to obtain different tool wear patterns and workpiece surface profiles. The machining time was between 0 and 5 min in dry cutting.

3 Methodology

3.1 Input variables and determination of experiment size using DOE method

Figure 2 shows the various stages of the algorithm used to predict the average surface roughness (R_a) and the dimensional deviation (D_d) of the workpiece. In stage 1, the appropriate size of the experiment was determined using *Design-Expert* software (version 6.0.7) based on DoE. The input variables, i.e., cutting speed, feed rate, depth of cut, and duration of machining, were organized in three levels, i.e., −1 for minimum value, 0 for center value, and +1 for maximum value. Previous studies have shown that cutting tool geometry, cutting speed, feed rate, depth of cut, and tool wear have significant effects on the surface quality [5, 14–17]. Table 1 shows the machining variables used to design the experiments at different variable levels.

3.2 Capturing and digital processing of images

In stage 2, the CCD camera was used to capture a 2-D image of the nose area of the cutting tool and an edge profile of the workpiece intermittently during machining. The tool was moved away from the freshly cut surface and the lathe was switched off before capturing the images. Compressed air was used to blow off dirt and chips adhering to the surface of the workpiece and cutting tool. In stage 3, *Wiener* filtering was used to recover the images that were affected by noise. In stage 4, the images were segmented to separate the object (dark region) from the background (bright region) using Otsu's thresholding

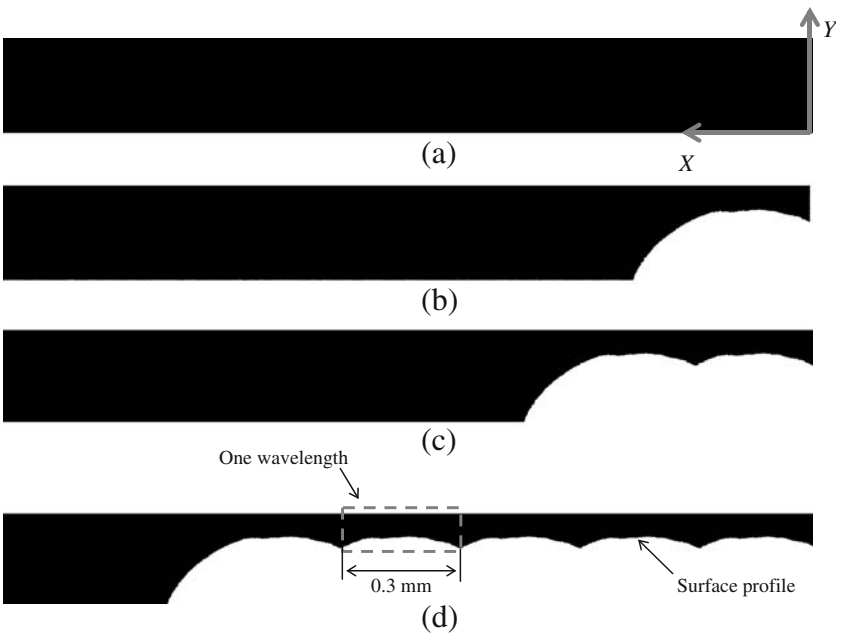

Fig. 5 Image of surface profile of simulated workpiece **a** before machining, **b** after one "rotation" of machine spindle, **c** two "rotations" of machine spindle, and **d** five "rotations" of machine spindle using a worn cutting tool

method [18]. Detailed descriptions of the image processing stages can be found in our previous paper [19]. Figure 3a and b show the 2-D images of unworn (new) and worn cutting tools.

3.3 Simulation of surface profile of workpiece

The depth of cut was chosen smaller than 0.25 mm in order to study the surface quality of the workpiece in a finish turning operation, where the cutting process uses only the nose area of the cutting tool. In stage 5, a region of interest (ROI) in the nose area was cropped automatically. The black pixels (intensity 0) in the nose area (Fig. 3c) were inverted to white (intensity 1), while the white pixels were inverted to black, as shown in Fig. 3d, so that the image can be used for generating the workpiece profile.

In a turning operation, the surface profile of the workpiece is created periodically due to the interaction between the tool feed and workpiece rotation. The wavelength of the waviness pattern on the surface is equal to the feed per revolution of the spindle. The combination of the cutting tool movement and the workpiece rotation produces a helical pattern as in Fig. 4. The figure shows that the flank wear land in zone B located on the major cutting edge (VB_B) does not affect the surface roughness of the workpiece, whereas the flank wear land in zone C (VB_C) affects the roughness significantly due to its direct contact with the freshly cut surface.

In stage 6, a black rectangle (intensity 0) was created to simulate the unmachined workpiece as in Fig. 5a. The height and the length of the rectangle are two optional parameters defined in the initial part of the *Matlab* program developed to generate the simulated surface. The height of the black rectangle is equal to the height of the cutting tool image cropped in stage 5, and the length is equal to five times the feed. The inverted image of the cutting tool in Fig. 3d was added pixel-by-pixel to the black rectangle. Figure 5b shows the result of this process. The surface profile of the simulated "workpiece" was generated in this manner by moving the reference point along the surface in steps of 0.3 mm (equivalent to 322 pixels) for a feed rate of 0.3 mm/rev. Figure 5b–d show one wavelength, two wavelengths, and five wavelengths of surface profile simulated using this method, respectively. This is equivalent to one, two, and five rotations of a real workpiece. It was necessary to replicate the profile in this manner so that at least two peaks occur within the sampling length [20]. This process generates a simulated digital image of the

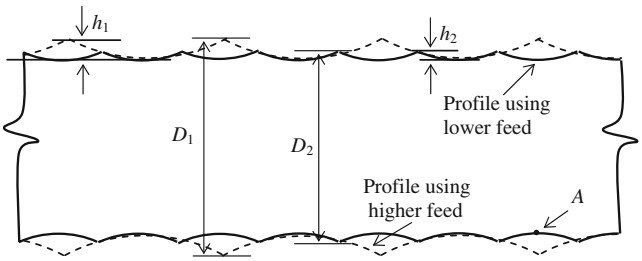

Fig. 6 Schematic of superimposed simulated workpiece profiles for feed rates f_1 and f_2

Table 2 Machining parameters designed using DoE

Test no.	Machining duration (min)	Feed rate (mm/rev)	Cutting speed (m/min)	Depth of cut (mm)
1	0	0.20	170	0.15
2	0	0.30	170	0.15
3	0	0.20	206	0.15
4	0	0.30	206	0.15
5	0	0.25	188	0.20
6	0	0.20	170	0.25
7	0	0.30	170	0.25
8	0	0.20	206	0.25
9	0	0.30	206	0.25
10	2.5	0.25	188	0.15
11	2.5	0.25	170	0.20
12	2.5	0.20	188	0.20
13	2.5	0.25	188	0.20
14	2.5	0.25	188	0.20
15	2.5	0.25	188	0.20
16	2.5	0.25	188	0.20
17	2.5	0.25	188	0.20
18	2.5	0.25	188	0.20
19	2.5	0.30	188	0.20
20	2.5	0.25	206	0.20
21	2.5	0.25	188	0.25
22	5.0	0.20	170	0.15
23	5.0	0.30	170	0.15
24	5.0	0.20	206	0.15
25	5.0	0.30	206	0.15
26	5.0	0.25	188	0.20
27	5.0	0.20	170	0.25
28	5.0	0.30	170	0.25
29	5.0	0.20	206	0.25
30	5.0	0.30	206	0.25

Table 3 Machine tool and other parameters

Machine tool	Conventional lathe machine (Pinacho S90/200, Spain)
Workpiece	Alloy steel rod, AISI 304
Coolant	Air
Cutting tool	Cemented carbide: CNGP-12-04-04_H13A (Sandvik, Sweden)

Fig. 7 Comparison between images of real workpieces (*left*) and images of simulated workpiece using cutting tool image (*right*). **a** Sample no. 8. **b** Sample no. 16. **c** Sample no. 23

Table 4 Comparison between average roughness ($R_{a(r)}$) and dimensional deviation ($D_{d(r)}$) for real workpiece (measured) and the corresponding values determined from simulated images ($R_{a(s)}$ and $D_{d(s)}$)

Sample no.	Average roughness values R_a				Dimensional deviation			
	$R_{a(r)}$ (μm)	$R_{a(s)}$ (μm)	$\Delta R_{a(r,s)}$ (μm)	$\Delta R_{a(r,s)}$ %	$D_{d(r)}$ (μm)	$D_{d(s)}$ (μm)	$\Delta D_{d(r,s)}$ (μm)	$\Delta D_{d(r,s)}$ %
1	4.3	4.2	0.1	2.3	35	32	3	8.6
2	7.5	7.8	0.3	4	60	58	2	3.3
3	4.8	4.5	0.3	6.2	34	32	2	5.9
4	7.7	7.6	0.1	1.3	57	54	3	5.3
5	5.6	5.8	0.2	3.6	40	44	4	10
6	4.5	4.2	0.3	6.7	35	32	3	8.6
7	7.4	7.6	0.2	2.7	55	56	1	1.8
8	4.5	4.3	0.2	4.4	32	30	2	6.3
9	7.8	8.1	0.3	3.8	60	58	2	3.3
10	6.4	5.9	0.5	7.8	45	44	1	2.2
11	6.2	6.1	0.1	1.6	39	36	3	7.7
12	4.1	4.4	0.3	7.3	32	34	2	6.3
13	5.8	6	0.2	3.4	46	44	2	4.3
14	6	5.8	0.2	3.3	46	42	4	8.7
15	6.3	6.1	0.2	3.2	48	44	4	8.3
16	5.7	6	0.3	5.3	46	50	4	8.7
17	6.3	6	0.3	4.8	48	46	2	4.2
18	6.1	6.2	0.1	1.6	45	46	1	2.2
19	7.6	7.6	0	0	67	64	3	4.5
20	6.4	5.9	0.5	7.8	48	46	2	4.2
21	5.7	5.5	0.2	3.5	46	44	2	4.3
22	4.3	4.4	0.1	2.3	36	34	2	5.6
23	8.1	8.3	0.2	2.5	57	56	1	1.8
24	1.9	2.1	0.2	10.5	13	14	1	7.7
25	1.1	1.2	0.1	9.1	12	12	0	0
26	6.8	6.5	0.3	4.4	50	52	2	4
27	4.3	4.4	0.1	2.3	30	32	2	6.7
28	7.2	7	0.2	2.8	51	48	3	5.9
29	1.6	1.8	0.2	12.5	16	14	2	12.5
30	1.0	0.9	0.1	10	11	10	1	9.1

$\Delta R_{a(r,s)} = \left|R_{a(r)} - R_{a(s)}\right|$ $\Delta R_{a(r,s)}\% = \left|\frac{R_{a(r)} - R_{a(s)}}{R_{a(r)}}\right| \times 100$ $\Delta D_{d(r,s)} = \left|D_{d(r)} - D_{d(s)}\right|$ $\Delta D_{d(r,s)}\% = \left|\frac{D_{d(r)} - D_{d(s)}}{D_{d(r)}}\right| \times 100$

workpiece profile in turning when the tool cuts the workpiece at a known feed rate.

The pixel-by-pixel addition of the tool image to the simulated workpiece produces an image similar to the surface profile of the workpiece in an actual machining operation and is given by:

$$f_5(x,y) = f_4(x,y) + f_3(x,y), \quad (1)$$

where

f_3 (x, y) is the image of the cutting tool from stage 6 of the algorithm.
f_4 (x, y) is the image of simulated workpiece before "machining" (f_4 (x, y)=0).
f_5 (x, y) is the simulated surface profile of workpiece after "machining".

The distance between each tool image added to the uncut "workpiece" image is equal to the feed in the x direction (along the axis), while the depth of the image overlap depends on the depth of cut in the real machining. The scaling factors obtained by calibration were used to convert the actual feed and depth-of-cut from millimeters to pixels because the simulated images have dimensions in pixels. Figure 5d shows the image of one side of the surface profile of the simulated workpiece generated using the image of a worn cutting tool for feed of 0.3 mm/rev. In stage 7 of the algorithm, the simulated surface profile was cropped to evaluate the average surface roughness. The cut-off distance for roughness measurement was 0.8 mm for feed rates of 0.2, 0.25, and 0.3 mm/rev based on the BS1134-2 (1990) standard [21]. The scaling factors were used to change the cut-off from millimeters to pixels.

3.4 Surface roughness measurement from simulated workpiece

In stage 8, the profile of the simulated surface was extracted using the algorithm published in our previous work [22] and was used to find the roughness value. In stage 9, the average roughness (R_a) value was determined by subtracting each point on the profile from its mean line. If equal spaces of horizontal distances, assumed as 1, 2, … n, have absolute heights h_1, h_2, ... h_n, respectively, then R_a is given by:

$$R_a = \frac{|h_1| + |h_2| + |h_3| + \ldots + |h_n|}{n} = \frac{1}{n}\sum_{i=1}^{n} |h_i| \quad (2)$$

The accuracy of the average roughness extracted from a 2-D profile of a real workpiece was verified with a stylus-type roughness tester and found to be within 10% [22].

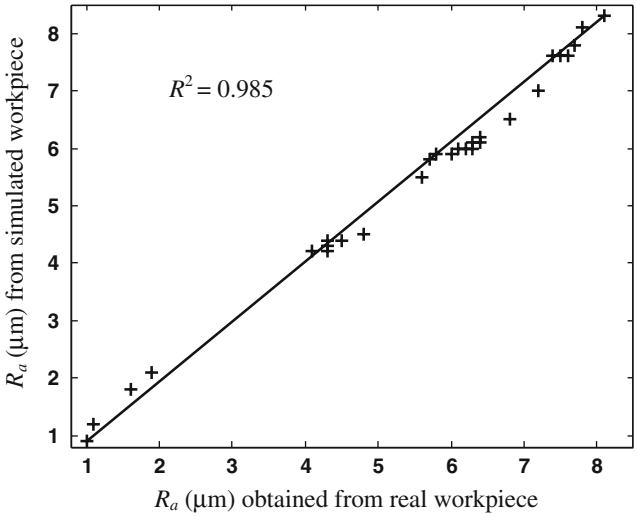

Fig. 8 Comparison between average roughness R_a from real and simulated workpiece images

3.5 Determination of the dimensional deviation (D_d) of simulated workpiece

In stage 10, the profile of the simulated workpiece was used to determine the dimensional deviation D_d (labeled as $D_{d(s)}$) caused by different feeds. Figure 6 shows a schematic of the superimposed profiles for two different feeds (f_1 and f_2) machined using a new tool. The difference between maximum heights of two superimposed surface profiles D_d gives the dimensional deviation of workpiece due to the two different feed rates, i.e.,

$$D_d = D_1 - D_2 = 2(h_1 - h_2), \quad (3)$$

where D_1 and D_2 are the outside diameters of the workpiece machined using feed f_1 and f_2, respectively, and h_1 and h_2 are the maximum heights of two surface profiles (using f_1

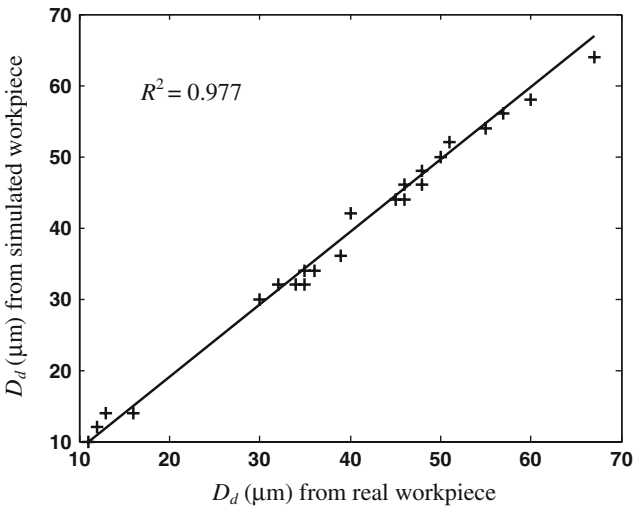

Fig. 9 Comparison between D_d from real and simulated workpiece

Table 5 Comparison between average roughness ($R_{a(a)}$) and dimensional deviation ($D_{d(a)}$) from approximation models and corresponding values ($R_{a(r)}$ and $D_{d(r)}$) from direct measurement on real workpieces

Sample no.	$R_{a(r)}$ (μm)	$R_{a(a)}$ (μm)	$\Delta R_{a(r,a)}$ (μm)	$\Delta R_{a(r,a)}$ %	$D_{d(r)}$ (μm)	$D_{d(a)}$ (μm)	$\Delta D_{d(r,a)}$ (μm)	$\Delta D_{d(r,a)}$ %
1	4.3	4.2	0.1	2.3	35	32.6	2.4	6.9
2	7.5	7.8	0.3	4	60	58.1	1.9	3.2
3	4.8	4.5	0.3	6.2	34	32	2	5.9
4	7.7	7.6	0.1	1.3	57	54.5	2.5	4.4
5	5.6	5.7	0.1	1.8	40	42.6	2.6	6.5
6	4.5	4.2	0.3	6.7	35	32.1	2.9	8.3
7	7.4	7.6	0.2	2.7	55	56.6	1.6	2.9
8	4.5	4.3	0.2	4.4	32	30.5	1.5	4.7
9	7.8	8.1	0.3	3.8	60	58	2	3.3
10	6.4	5.8	0.6	9.4	45	42.6	2.4	5.3
11	6.2	6	0.2	3.2	39	34.6	4.4	11.3
12	4.1	4.3	0.2	4.9	32	32.6	0.6	1.9
13	5.8	6.1	0.3	5.2	46	46.8	0.8	1.7
14	6	6.1	0.1	1.7	46	46.8	0.8	1.7
15	6.3	6.1	0.2	3.2	48	46.8	1.2	2.5
16	5.7	6.1	0.4	7	46	46.8	0.8	1.7
17	6.3	6.1	0.2	3.2	48	46.8	1.2	2.5
18	6.1	6.1	0	0	45	46.8	1.8	4
19	7.6	7.5	0.1	1.3	67	62.6	4.4	6.6
20	6.4	5.8	0.6	9.4	48	44.6	3.4	7.1
21	5.7	5.4	0.3	5.3	46	42.6	3.4	7.4
22	4.3	4.4	0.1	2.3	36	34	2	5.6
23	8.1	8.3	0.2	2.5	57	56.5	0.5	0.9
24	1.9	2.1	0.2	10.5	13	14.4	1.4	10.8
25	1.1	1.2	0.1	9.1	12	11.9	0.1	0.8
26	6.8	6.4	0.4	5.9	50	50.6	0.6	1.2
27	4.3	4.4	0.1	2.3	30	32.5	2.5	8.3
28	7.2	7	0.2	2.8	51	48	3	5.9
29	1.6	1.8	0.2	12.5	16	13.9	2.1	13.1
30	1	0.9	0.1	10	11	10.4	0.6	5.5

$\Delta R_{a(r,a)} = |R_{a(r)} - R_{a(a)}|$, $\Delta D_{d(r,a)} = |D_{d(r)} - D_{d(a)}|$

and f_2), respectively. The maximum heights (h_1 and h_2) were determined from the simulated profile. The dimensional deviation obtained from the simulated surface was compared with that measured from the real workpiece using a 1-μm-resolution micrometer (Mitutoyo, model 293-153-30) with an accuracy of ±1 μm.

3.6 Modeling and prediction of surface roughness and dimensional deviation using response surface method (RSM)

The response surface method (RSM) is a statistical method used to model and analyze problems in which several variables affect the response of interest. RSM is usually used when the optimization of output response is the objective of the study. The process yield is the output parameter (y) via the input variables such as cutting speed (x_1), feed rate (x_2), depth of cut (x_3), and duration of machining (x_4), which can be written as:

$$y = f_1(x_1, x_2, x_3, x_4) + \varepsilon_1, \tag{4}$$

where ε_1 represent the noise or error of the response y.

If the expected response is given by

$$E(y) = f(x_1, x_2, ...), \tag{5}$$

then the response surface η is

$$\eta = f(x_1, x_2, ...) \tag{6}$$

RSM is based on the regression method to find an approximation surface that is best fitted to the data. The

equation of this surface should be able to model the responses of interest using the independent variables (x_1, x_2, ...). The second-order or third-order models are more complex than first-order models to analyze the relationship between input variables and output parameters. However, the first-order model is not always a suitable approximation as a true function to correlate the input variables (x_1, x_2, ..., x_k) and output values (y_1, y_2, ..., y_k). Therefore, a second- or third-order model is used to find a suitable approximation model. The second-order approximation function y is given by

$$y = \beta_0 + \sum_{i=1}^{k} \beta_i x_i + \sum_{i=1}^{k} \beta_{ii} x_i^2 + \sum_{i<j} \sum \beta_{ij} x_i x_j + \varepsilon, \qquad (7)$$

where β_0, β_i, β_{ii}, and β_{ij} are the coefficients of approximation of second-order function, x_i and x_j are the input variables, and k is the number of input variables.

The relationship between the responses and the input variables is usually assessed using the statistical parameter R^2 value [23]. A value of R^2 closer to unity is desirable, indicating a good fit. In stage 11, the average roughness $R_{a(s)}$ and dimensional deviation $D_{d(s)}$ of simulated workpieces obtained from stage 9 and stage 10 were used as the response values to determine the approximation model.

4 Results and discussion

This section consists of three subsections. In subsection 4.1, the average roughness and dimensional deviation obtained using the approximation model, simulated images, and the actual values measured using the conventional methods are compared. In sub-section 4.2, five tests were repeated, and the data obtained using the simulated images are compared with those obtained using the approximation models. In subsection 4.3, an attempt to optimize the output response using RSM for a given range of input parameters is described.

4.1 Modeling and prediction of surface roughness and dimensional deviation using 2-D images of cutting tool and RSM

Several workpieces under different machining conditions determined using DoE were machined using uncoated cutting tools to develop the RSM models for R_a and D_d. The combinations of machining parameters in the DoE were obtained using *Design-Expert* (version 6.0.7) software and are shown in Table 2. When the cutting tools were used to machine samples 1 to 9, the machining durations were about 3 to 4 s. Thus, the machining durations for these samples were not exactly 0 min as shown in the table. Also, the deviation in machining duration for samples 10 to 30 is about ±2 s. However, for simplicity, the machining durations were rounded to 0, 2.5, and 5 min. Table 3 gives the other machining parameters.

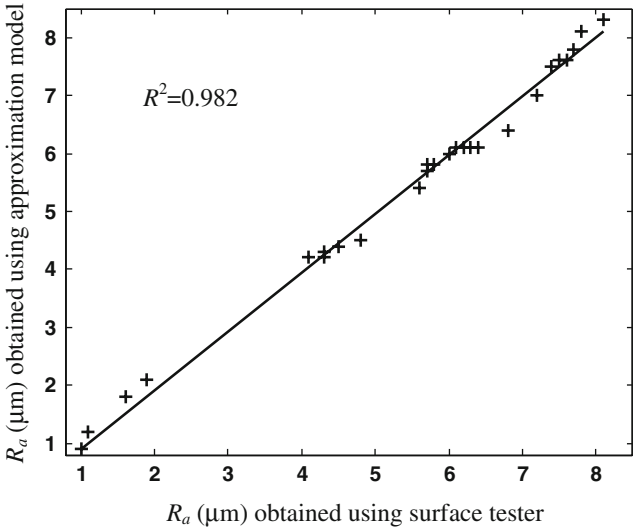

Fig. 10 Comparison the R_a values between results using surface roughness tester and approximation model

The images of cutting tools and surface profiles of workpieces were captured for each combination of machining parameters in Table 2. The image of the tool shows the nose area affected by nose wear. The simulated surface profiles were generated using these images as outlined in section 3.3. Figure 7a–c compare the real and simulated surface profiles for three workpieces, where the tool images were chosen from test numbers 8, 16, and 23 in Table 2. Visual comparison between the surface profiles of simulated workpieces generated using 2-D images of tools and the

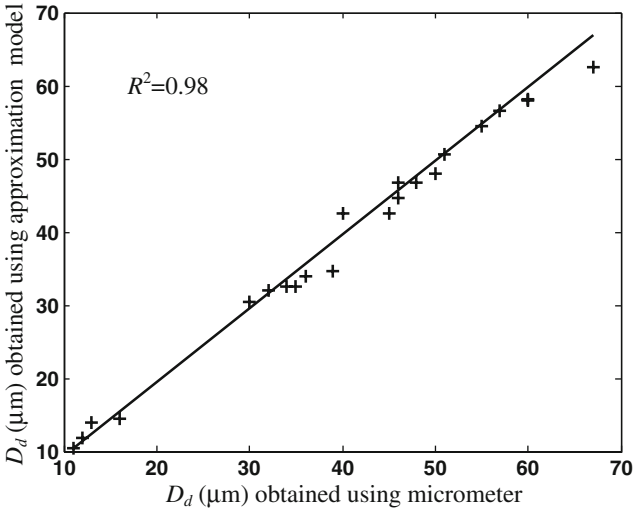

Fig. 11 Comparison the D_d values between results using micrometer and approximation model

Table 6 The random machining parameters used to verify the capability of approximation models

Sample no.	Machining time	Feed rate (mm/rev)	Cutting speed (m/min)	Depth-of -cut (mm)
11	2 min 30 s	0.25	170	0.20
12	2 min 30 s	0.20	188	0.20
15	2 min 30 s	0.25	188	0.20
20	2 min 30 s	0.25	206	0.20
28	5 min 0 s	0.30	170	0.25

real profile clearly shows their similarity. This shows that the workpiece profiles can indeed be generated using the 2-D profiles of the worn tool, thus enabling various feed rates and depths of cut to be easily experimented on with while generating the images.

The surface roughness $R_{a(r)}$ and dimensional deviation $D_{d(r)}$ for each real workpiece in Table 2 were measured using a stylus-type surface tester (Mitutoyo, model SJ-201P) and a 1-μm-resolution micrometer, respectively. The corresponding values for the simulated workpieces ($R_{a(s)}$ and $D_{d(s)}$) were also determined using the algorithm. The results are shown in Table 4. The differences in surface roughness ($\Delta R_{a(r,s)}$) and dimensional deviation ($\Delta D_{d(r,s)}$) between the real and simulated images are also shown in the same table. The mean and standard deviation in the differences for $\Delta R_{a(r,s)}$ from 30 results are 0.21 and 0.11 μm, respectively. Meanwhile, the mean and standard deviation in the differences for $\Delta D_{d(r,s)}$ are 2.2 and 1.03 μm, respectively. Expressed as a percentage of the values measured on the real surface, the mean difference in average roughness from the 30 tests is 4.7%, thus showing that the accuracy of the roughness measured using the profile of the simulated workpiece is acceptable. The occasional large differences (e.g., samples 24, 29, and 30) could be due to several factors, including machine harmonics. Also, the mean difference (in percentage) in dimensional deviation between measurement from the real workpiece and the simulated profile is 5.7%. The small difference also shows that the proposed method is suitable for evaluating the dimensional deviation D_d using the simulated workpiece.

Figure 8 compares the $R_{a(r)}$ and $R_{a(s)}$ values and Fig. 9 compares the $D_{d(r)}$ and $D_{d(s)}$ values for the 30 samples. The R^2 values were 0.985 and 0.977 for roughness and dimensional deviation, respectively. The close correlation indicates that the differences between the values obtained from the real workpieces and those obtained using the simulated images are small.

In the next step, the tool box of RSM in *Design-Expert* was used to generate two mathematical models that relate the input variables (duration of machining, feed rate, cutting speed, and depth-of-cut) and output parameters, namely average, roughness and dimensional deviation. The $R_{a(s)}$ and $D_{d(s)}$ values from the simulated workpieces (Table 4) were used as the output parameters, while the input parameters are as given in Table 2.

For the second-order approximation model, the initial results showed that the difference between the predicted output and those obtained from direct measurement ($R_{a(r)}$ and $D_{d(r)}$) was found to be up to 30%. Due to the large difference, the third-order model was finally adopted. The R^2 parameters for the third-order model were 0.997 for average roughness and 0.989 for dimensional deviation, indicating a good fit. The equations for the approximation models for predicting average roughness ($R_{a(a)}$) and dimensional deviation ($D_{d(a)}$), respectively, are given by

$$\begin{aligned} R_{a(a)} = {} & 6.14 + 0.35t + 1.6f - 0.1c - 0.2d - 0.119t^2 \\ & - 0.269f^2 - 0.269c^2 - 0.569d^2 - 0.575tf \\ & - 1.18tc - 0.125td - 0.525fc - 0.05fd \\ & + 0.075cd - 0.437t^2f - 0.988t^2c \\ & + 0.0875t^2d - 1.49tf^2 - 0.513tfc - 0.113tfd \\ & + 0.0125tcd + 0.137fcd \end{aligned} \quad (8)$$

Table 7 Comparison of average surface roughness between results obtained from approximation model and measurement on image of real workpieces

Sample no.	$R_{a(s)}$ (μm)	$R_{a(a)}$ (μm)	$\Delta R_{a(s,a)}$ (μm)	$\Delta R_{a(s,a)}$ (%)
11	6.5	6	0.5	7.7
12	3.8	4.3	0.5	13.2
15	5.7	6.1	0.4	7.0
20	6.4	5.8	0.6	9.4
28	6.5	7	0.5	7.7
Mean of differences			0.5	9.0

$$\Delta R_{a(s,a)} = \left|R_{a(s)} - R_{a(a)}\right|,$$

$$\Delta R_{a(s,a)}(\%) = \left|\frac{R_{a(s)} - R_{a(a)}}{R_{a(s)}}\right| \times 100$$

Table 8 Comparison of dimensional deviation between predictions of approximation model and results obtained from real images of workpieces

Sample no.	$D_{d(s)}$ (μm)	$D_{d(a)}$ (μm)	$\Delta D_{d(s,a)}$ (μm)	$\Delta D_{d(s,a)}$ % (μm)
11	30.1	34.6	4.5	15.0
12	36.3	32.6	3.7	10.2
15	50.9	46.8	4.1	8.1
20	40	44.6	4.6	11.5
28	42.7	48	5.3	12.4
Mean of differences			4.4	11.4

$$\Delta D_{d(s,a)} = \left|D_{d(s)} - D_{d(a)}\right|,$$
$$\Delta D_{d(s,a)}(\%) = \left|\frac{D_{d(s)} - D_{d(a)}}{D_{d(s)}}\right| \times 100$$

$$\begin{aligned} D_{d(a)} = {} & 46.8 + 4t + 15f + 5c - 0.000d - 0.211t^2 \\ & + 0.789f^2 - 7.21c^2 - 4.21d^2 - 4.25tf \\ & - 7.25tc - 0.75td - 2.75fc - 0.25fd \\ & + 0.75cd - 6.75t^2f - 12.8t^2c - 0.75t^2d \\ & - 12.3tf^2 - 2.75tfc - 0.75tfd + 0.25tcd \\ & + 0.75fcd, \end{aligned} \quad (9)$$

where t is the duration of machining, f is the feed, c is the cutting speed, and d is the depth of cut, as in Table 1 (all are coded values). The coefficients of the coded variables show which variable affects the output parameter significantly. The equations can be used to predict the roughness and dimensional deviation if the input values are known.

Equation 8 shows that feed rate affects the surface roughness of the workpiece significantly because the coefficient of f (1.6) is larger than the coefficient of t, c, and d. The published reports of other researchers also showed the importance of feed rate on R_a [14, 24, 25]. Meanwhile, the equation shows that cutting speed alone does not affect the surface roughness significantly because the coefficient of c is only about 0.1. The results published in the literature agree on the effect of cutting speed on the surface roughness of the workpiece where the duration of machining is fixed. The papers published by Ozel and Karpat [24] and Choudhury and Bartarya [16], where the same duration of machining was used to study the effect of machining parameters on R_a, showed that the effect of cutting speed on R_a is not significant. However, the combination of t and c affects the surface roughness significantly because the coefficient of tc is 1.18 and coefficient of t^2c is 0.988. Fang and Dewhurst [25] reported that the cutting speed affects R_a when the machining process was carried out for different machining durations, i.e., t was not fixed. The results obtained for different durations of machining (0, 2.5, and 5 min) in this study agree with their findings. Thus, it can be concluded that, for the same duration of machining, cutting speed does not affect the average roughness R_a significantly, but it affects R_a when different durations of machining are used due to the different amounts of tool wear. Also, the equation

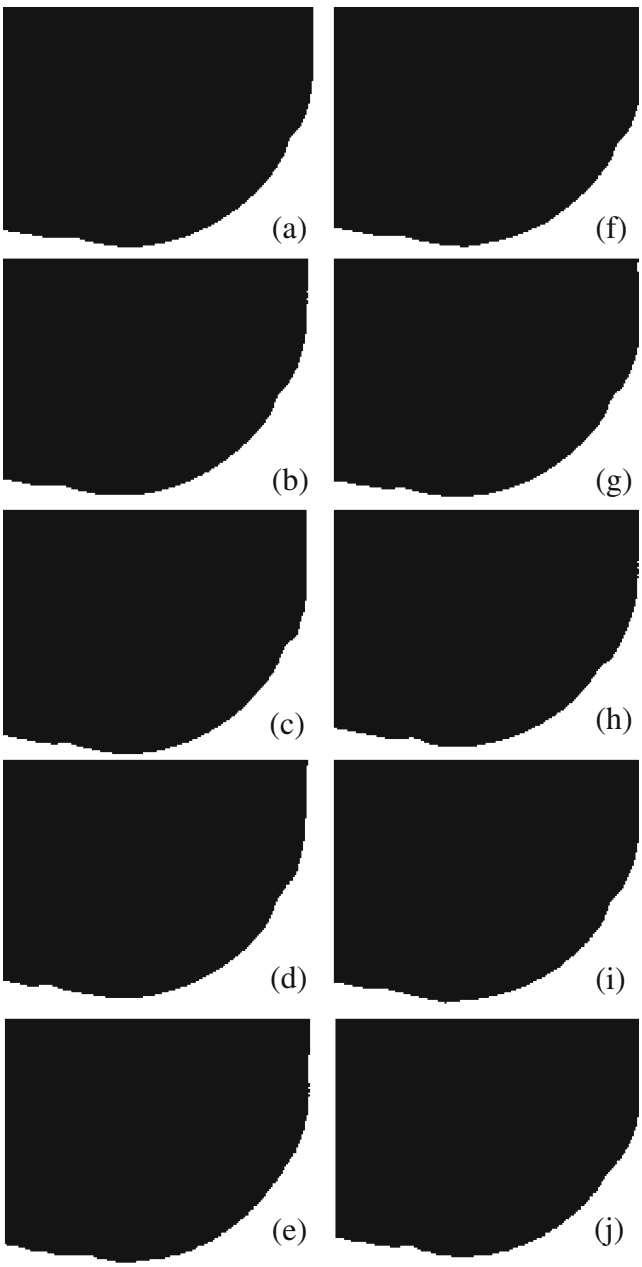

Fig. 12 Comparison between the binarized images of cutting tools described in: **a**–**e** sub-section 4.2 (samples 11, 12, 15, 20, and 28, respectively) and **f**–**j** sub-section 4.1 (samples 11, 12, 15, 20, and 28, respectively)

shows that a combination of t and f^2 affects R_a significantly. Thus, feed affects R_a alone or in combination with duration of machining. However, the depth of cut does not affect R_a significantly. This agrees with the results published by Jiao et al. [26].

Equation 9 shows that the effect of feed rate on the dimensional deviation of the workpiece is greater compared to the other variables. However, the coefficients in the equation show that the combination of machining duration and cutting speed affects the dimensional deviation greatly. The effect of variable d on the dimensional deviation is also not significant. Thus, Eqs. 8 and 9 show that the effect of machining duration, feed rate, cutting speed, and depth of cut on R_a and D_d more and less follow the same trend.

The predicted values for $R_{a(a)}$ and $D_{d(a)}$ from Eqs. 8 and 9 are shown in Table 5 for all the 30 samples and were compared with the values obtained by direct measurement on the real workpiece. Figures 10 and 11 show that values of R_a and D_d from the approximation models and those from direct measurement are close because of the high R^2 values. The absolute difference $\Delta R_{a(r,a)}$ between R_a obtained using stylus roughness tester and the approximation model are also shown in the table. The mean and the standard deviation of these differences are 0.22 and 0.14 μm, respectively. Also, the mean and the standard deviation for $\Delta D_{d(r,a)}$ are 1.91 and 1.12 μm, respectively. The corresponding mean deviation in percentage for $\Delta R_{a(r,a)}$ is 4.8%, while that for $\Delta D_{d(r,a)}$ (%) is 5.1%.

The small mean and standard deviations values for $\Delta R_{a(r,a)}$ and $\Delta D_{d(r,a)}$ from the 30 data show that the relationship between the input variables and output variables can be modeled accurately using the RSM developed using data extracted from the simulated workpiece surface. Thus, the 2-D images of cutting tools can be used to simulate the workpieces from which surface roughness and dimensional deviation can be determined, i.e., it is not necessary to extract the data from the actual workpiece in developing the models.

4.2 Comparison between prediction of approximation models and measurement from real images in a repeated run

The mathematical models in Eqs. 8 and 9 can be used for predicting the surface roughness and dimensional deviation of the workpiece when the machining parameters are known. In order to verify the capability of the approximation models in predicting these values, a new set of tests was arranged randomly among the 30 experiments shown in Table 2. Table 6 shows the tests chosen by using random sampling. The new set of experiments based on the data was carried out and the image of cutting tool for each test was captured in-cycle.

The values of $R_{a(r)}$ and $D_{d(r)}$ determined from the images of real workpiece profiles in the new set of experiments were compared to those predicted by the models (Tables 7 and 8). The binarized images of cutting tools (for test numbers 11, 12, 15, 20, and 28) are shown in Fig. 12a–e. Similar images of cutting tools used in the study described in sub-section 4.1 to develop the approximation models are shown in Fig. 12f–j. Comparison between the two sets of images shows that tool wear pattern under the same machining condition is not exactly the same, although the machining was repeated. This is suspected to be due to the non-homogeneous characteristics of cutting tool and workpiece that affect the surface profile, and also due to random vibration during cutting. Thus, the values of $R_{a(r)}$ and $D_{d(r)}$ can be expected to be slightly different from those predicted by the mathematical models ($R_{a(a)}$ and $D_{d(a)}$) generated with a different set of cutting tool images.

The data predicted by the models, i.e., $R_{a(a)}$ and $D_{d(a)}$, for the new set of experiments are also shown in Table 7 and 8. The mean difference of average roughness between the values obtained using the real images and those predicted by the approximation model ($\Delta R_{a(s,a)}$) is 9% (Table 7). Also, the mean difference of dimensional deviation ($\Delta D_{d(s,a)}$) between the real images and the approximation model is

Table 9 The optimized machining variables

Variables set no.	Machining time	Feed rate (mm/rev)	Cutting speed (m/min)	Depth of cut (mm)	R_a (μm)
1	9 min 28 s	0.30	182	0.186	3.14
2	9 min 01 s	0.29	184	0.204	3.46
3	9 min 59 s	0.29	185	0.201	3.02
4	8 min 49 s	0.27	189	0.226	3.94
5	8 min 23 s	0.30	183	0.195	3.87
6	8 min 20 s	0.26	192	0.247	3.53
7	8 min 32 s	0.29	187	0.217	3.21
8	9 min 29 s	0.26	191	0.238	3.15
9	9 min 23 s	0.24	192	0.249	3.98
10	9 min 11 s	0.30	182	0.191	3.94

11.4% (Table 8). These results show that the models can predict the surface roughness (R_a) and dimensional deviation (D_d) reasonably well. Thus, the surface profile of the workpiece can be generated using the 2-D images of the cutting tool alone to determine the parameters required to develop the model. It is not necessary to measure the values of R_a and D_d directly from the real workpiece to generate the models. When only new cutting tools are considered or if the tool wear is negligible, the values of R_a and D_d can be obtained even without actual machining.

The small difference between the results from the real images of the workpiece and the approximation model are suspected to be due to inaccuracy and instability of the lathe machine during machining. Part of this deviation could also be due to non-homogenous workpiece and cutting tool materials. The limited resolution of the CCD camera used, which was about 1 μm/pixel, could be another reason for this deviation. Also, the results obtained from 12 different samples produced using the conventional lathe machine showed that the deviation in the values R_a and D_d (in different locations of one sample) can vary up to 8.6% and 12.9%, respectively. Thus, use of a higher-resolution CCD camera and a more stable and accurate lathe machine is recommended to increase the accuracy of the results.

4.3 Optimization of the roughness value using RSM

Optimization of the output response is one of the goals of RSM. To achieve this, the range of desirable output responses and duration of machining were defined using *Design-Expert* software. The range for R_a was set arbitrarily between 3 and 4 μm. Also, the time of machining was limited between 8 and 10 min. These ranges were defined in order to control the surface quality of the workpiece. Ten groups of machining variables to fulfill the desirable output responses were obtained using *Design-Expert* software and are shown in Table 9. Use of each series of machining variables shown in Table 9 should give the desired R_a values. The results show that the RSM models can be used to predict suitable values of feed rate, cutting speed, and depth of cut to obtain a desirable surface quality. The results also show that the values of R_a can be controlled using the proposed method to attain the required surface quality, which is one of the important aims of finish turning.

5 Conclusion

This study has shown that data extracted from images of a workpiece that are digitally simulated using the 2-D profile of cutting tools can be used for generating mathematical models to predict the average roughness and dimensional deviation of the turned workpiece. Unlike previous work on the prediction of surface roughness in turning, where data extracted from the actual workpieces were used for developing the models, the proposed method requires only an image of the cutting tool to obtain the required data. By using an image of the tool, the workpiece profiles corresponding to different feed rates can be simulated, from which roughness and dimensional deviation can be determined. This removes the tedium associated with actual machining of the workpiece for different feed rates and direct measurement of roughness and dimensional deviation. The mathematical models developed were successfully used to predict the average roughness and dimensional deviation in randomized cutting operations.

Acknowledgement The authors would like to thank Universiti Sains Malaysia for the offer of the short-term grant that enabled this work to be carried out.

References

1. Benardos PG, Vosniakos GC (2003) Predicting surface roughness in machining: a review. Int J Mach Tools manuf 43:833–844
2. Lu C (2008) Study on prediction of surface quality in machining process. J Mater Process Technol 205:439–450
3. Cakir MC, Ensarioglu C, Demirayak I (2009) Mathematical modeling of surface roughness for evaluating the effects of cutting parameters and coating material. J Mater Process Technol 209:102–109
4. Choudhury IA, El-Baradie MA (1997) Surface roughness prediction in the turning of high-strength steel by factorial design of experiments. J Mater Process Technol 67:55–61
5. Arbizu IP, Pérez CJL (2003) Surface roughness prediction by factorial design of experiments in turning processes. J Mater Process Technol 143–144:390–396
6. Dabnun MA, Hashmi MSJ, El-Baradie MA (2005) Surface roughness prediction model by design of experiments for turning machinable glass–ceramic (Macor). J Mater Process Technol 164–165:1289–1293
7. Karayel D (2008) Prediction and control of surface roughness in CNC lathe using artificial neural network. J Mater Process Technol. doi:10.1016/ j.jmatprotec.2008.07.023
8. Risbood KA, Dixit US, Sahasrabudhe AD (2003) Prediction of surface roughness and dimensional deviation by measuring cutting forces and vibrations in turning process. J Mater Process Technol 132:203–214
9. Lee BY, Tarng YS (2001) Surface roughness inspection by computer vision in turning operations. Int J Mach Tools Manuf 41:1251–1263
10. Lee BY, Yu SF, Juan H (2004) The model of surface roughness inspection by vision system in turning. Mechatronics 14:129–141
11. Ho SY, Lee KC, Chen SS, Shinn-Ho J (2002) Accurate modeling and prediction of surface roughness by computer vision in turning operations using an adaptive neuro-fuzzy inference system. Int J Mach Tools Manuf 42:1441–1446
12. Lee K, Ho SJ, Ho SY (2005) Accurate estimation of surface roughness from texture features of the surface image using an adaptive neuro-fuzzy inference system. Precis Eng 29:95–100
13. Shahabi HH, Ratnam MM (2009) Non-contact roughness measurement of turned parts using machine vision. Int J Adv Manuf Tech. doi:10.1007/s00170-009-2101-0

14. Zhang JZ, Chen JC, Kirby ED (2007) Surface roughness optimization in an end-milling operation using the Taguchi design method. J Mater Process Technol 184(1–3):233–239
15. Castejon M, Alegre E, Barreiro J, Hernandez LK (2007) On-line tool wear monitoring using geometric descriptors from digital images. Int J Mach Tools Manuf 47:1847–1853
16. Choudhury SK, Bartarya G (2003) Role of temperature and surface finish in predicting tool wear using neural network and design of experiments. Int J Mach Tools Manuf 43:747–753
17. Suresh PVS, Rao PV, Deshmukh SG (2002) A genetic algorithmic approach for optimization of surface roughness prediction model. Int J Mach Tools Manuf 42:675–680
18. Otsu N (1979) A threshold delection method from gray-level histograms. IEEE Trans Syst Man Cybern 9(1):62–66
19. Shahabi HH, Ratnam MM (2007) On-line monitoring of tool wear in turning operation in the presence of tool misalignment. Int J Mach Tools Manuf 38(7–8):718–727
20. Smith GT (2002) Industrial metrology—surfaces and roundness. Springer, London
21. BS 1134-2 (1990) Assessment of surface texture. Part 2: guidance and general information, British Standard
22. Shahabi HH, Ratnam MM (2009) In-cycle monitoring of tool nose wear and surface roughness of turned parts using machine vision. Int J Mach Tools Manuf 40:1148–1157. doi:10.1007/s00170-008-1430-8
23. Montgomery DC (2005) Design and analysis of experiments. Wiley, New York
24. Ozel T, Karpat Y (2005) Predictive modeling of surface roughness and tool wear in hard turning using regression and neural networks. Int J Mach Tools Manuf 45:467–479
25. Fang N, Dewhurst P (2005) Slip-line modeling of built-up edge formation in machining. Int J Mech Sci 47:1079–1098
26. Jiao SL, Pei ZJ, Lee ES (2004) Fuzzy adaptive networks in machining process modeling: surface roughness prediction for turning operations. Int J Mach Tools Manuf 44:1643–1651